AUTHORIZATION TO LEND AND REPRODUCE THE THESIS

As the sole author of this thesis, I authorize Brown University to lend it to other institutions or individuals for the purpose of scholarly research.

Date _____ _____

Jianzhe Yang, Author

I further authorize Brown University to reproduce this thesis by photocopying or other means, in total or in part, at the request of other institutions or individuals for the purpose of scholarly research.

Date _____ _____

Jianzhe Yang, Author

Deep indentation contact experiments with nonlinear model fitting

By

Jianzhe Yang

B.E., China University of Mining and Technology (Beijing), 2015

A Dissertation submitted in partial fulfillment of the
requirements for the Degree of Master of Science
in the School of Engineering at Brown University

Providence, Rhode Island

May 2017

This thesis by

Jianzhe Yang

is accepted in its present form by

the School of Engineering

at

Brown University

as satisfying the thesis requirements for the degree of Master of Science.

Date _____ _____

Haneesh Kesari, Advisor

Approved by the Graduate Council

Date _____ _____

Andrew G. Campbell, Dean of the Graduate School

Vita

Jianzhe Yang was born in Henan Province, China. He received the B.E. in Mechanical Engineering and Automation from China University of Mining and Technology (Beijing) in 2015. Subsequently, he entered the Mechanics of Solids program at Brown University in the fall of 2015. His research focuses on experimental contact mechanics.

Acknowledgements

First, I would like to thank my advisor, Prof. Haneesh Kesari, for offering me his kind support as well as valuable guidance throughout all my years at Brown University. I have benefited greatly from his extensive expertise in mechanics and math. I also would like to thank all the professors at Brown with whom I have taken courses, and who introduced me to solid mechanics and selflessly shared their knowledge with me.

Second, I would like to express my gratitude to the members of the Applied Mechanics Lab. Special thanks to Michael Monn and Weilin Deng, for their valuable guidance and help in my graduate studies. And also I would like to thank Wenqiang Fang and Kaushik Vijaykumar for their academic help and advice.

Third, I want to thank my friends here in the U.S. and in China. Their support helped me get here. When I needed advice or understanding, they were always present and always solidly backed me up.

Finally, I want to thank my family, my parents and my sister. I could not have completed the program without their support and understanding.

Contents

List of Tables

List of Figures

Abstract

Over the past decades, the mechanical behavior of biological material has had a profound effect on research into human tissues and the development of medical devices. Studies from macrostructures to nanostructures of biological materials have been investigated. Experimental tools have been used to explore these mechanical properties. Soft material is one of the most widely found biological materials in nature. Understanding the mechanical behavior of soft material is important in order to develop cell mechanics and clinical devices. This thesis investigates the mechanical behavior of polydimethylsiloxane (PDMS) under large deformation by conducting deep indentation contact experiments. We use a long thin indenter to indent into three different PDMS samples to explore their strain behaviors under large deformation. We find the relationship between the loading force and the deformation of PDMS. A hysteresis is also found between the loading process and the unloading process. Three potential factors of viscoelasticity, friction and surface roughness are discussed.

CHAPTER 1

Introduction

An understanding of the mechanical properties of biological materials is critical for research and applications, including cell mechanics research, tissue modeling and the development of clinical devices. Macrostructures and nanostructures of biological materials have been studied to explore their mechanical properties in the recent two decades [**1, 2, 3, 4**].

Soft materials are widely found in organs and biological tissues [**5**]. The mechanical behavior of soft material is important for tissue mechanics studies, industry applications and medical devices. In recent years, much research has been conducted. For example, H. Saraf has investigated the soft human heart, lung and liver mechanical properties under dynamic loading [**6**]. Mechanical properties of bioactive materials have been studied by T. Kokubo [**7**].

However, it is still difficult to characterize elastic properties of soft biological materials due to sensitivity to environment and inhomogeneity [**8**]. Environment factors remarkably influence their mechanical properties. For instance, temperature may affect the performance of biomaterials on their elastic properties. I. Engelberg demonstrated that high temperature may reduce the flexural storage modulus of polymers [**9**]. Besides environment factors, inhomogeneity exists in many biomaterials. The local elastic properties of biomaterials are always different at different places and the mechanical behaviors vary a lot at different locations [**10**].

Indentation test is one of the most widely used methods to characterize materials' hardnesses and elastic moduli. It was originally invented to characterize the hardnesses of engineering materials, such as metals and composite materials. The testing system has become a standard and is widely used for engineering materials. Experiments have been conducted to determine the hardnesses and elastic moduli of

materials such as fused silica, aluminum and sapphire [**11**]. In the last two decades, indentation has been developed as an effective method to characterize biomaterials. Applications have been made to measure the elastic properties of human bones [**12**] and dentin [**13**]. Nanoindentation has also been applied to characterize soft gels [**14**].

Contact experiment is also a popular method to determine the compliant material properties such as elastic modulus and surface energy [**15**]. A sphere indenter is often used to contact and indent into the sample at a small depth. The loading force and displacement are measured to compute the mechanical properties. Hertz contact model, JKR and DMT theories are three of the most popular tools when dealing with elastic contact mechanics problems. For example, P. D. Warren used Hertzian indentation to explore the fracture toughnesses of glass and alumina [**16**]. KC Wu employed JKR method to determine solid material elastic modulus and surface energy [**17**]. Yifang Cao performed indentation to determine the initial contact and adhesion characteristics by applying JKR and DMT theories [**18**].

However, there two drawbacks of traditional indentation test method: first, the scale of deformation is very small, so we can not explore the mechanical behavior under large deformation, second, it does not work well for very soft material because the measuring scale is very small (nN-mN). Also, there are some limitations of JKR experiments, such as inability to calibrate hyperelastic models and sensitivity to geometry. What's more, investigating a bulk property of a large sample is not feasible using Hertz, JKR and DMT theories.

This thesis employs deep indentation contact experiments to investigate the mechanical behavior of PDMS under large deformation. We use a long thin indenter to indent into soft materials as deep as at least 5 times of its diameter. The loading force scale and the deformation scale are mN to N and μm to cm, respectively. The deep indentation shows the bulk property of PDMS under large deformation. S. Fakhouri has conducted puncture experiments on gels to explore the critical load for material failure and strain behavior described with a neo-hookean model using a similar testing method [**19**].

The work of this thesis is to use a long thin indenter to conduct deep indentations into soft PDMS samples. Three PDMS samples of different stiffnesses from $5kPa$ to $20kPa$ are used. We make the long thin indenter punch into the PDMS samples at around $10mm$ in depth.

The experimental results show that the force-deformation of PDMS has an exponential relationship under large deformation. We find a hysteresis between the loading and unloading process, the potential reasons of which are viscoelasticity, friction, roughness and others.

We conduct two sets of experiments to verify the influences of viscoelasticity, friction and roughness. The results demonstrate that the PDMS samples present a viscoelasticity behavior, which is commonly observed in the experiments [**20**]. Furthermore, as the indentation depth becomes larger than the diameter of the indenter, the surrounding PDMS would contact with the circumferential surface of the indenter, thus introducing friction force on the indenter. Lastly, as demonstrated by Haneesh and Deng, surface roughness and adhesion could also result in hysteresis caused by the small-scale contact instability [**21, 22, 23**]. Therefore, the surface roughnesses of the PDMS samples and the indenter are also potential factors for the observed hysteresis.

CHAPTER 2

Experiments

A custom-built mechanical testing system (MTS) is used to conduct deep indentation experiments as shown in Figure 2.1. The MTS is constructed based on the previous device setup by Jarod Ferreira [**24**]. Three sets of individual tests are conducted: a cantilever stiffness test, a rigid indentation test and three PDMS deep indentation tests. The first two sets determine the relationship between force and voltage and the relationship between displacement and voltage. From the last set, we collect the voltage data and determine the sample deformation. By doing a linear fitting, we know the stiffness of the cantilever. Multiply the cantilever stiffness and its displacement we can get the loading force. Finally, we obtain the force-deformation relationships of the PDMS samples.

The design principle of the MTS is as follows. As shown in Figure 2.1, a cantilever is fixed on the aluminum frame. Attached to the cantilever, a fiber optic displacement sensor (FODS) is applied to measure the displacement of the cantilever. Besides,

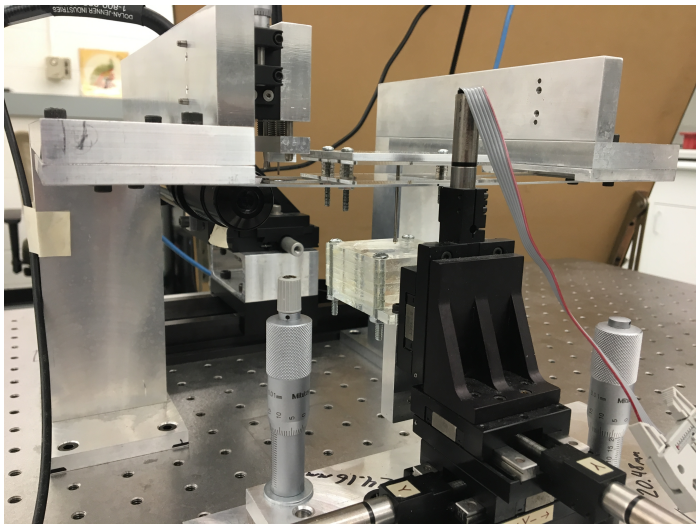

FIGURE 2.1. The custom-built mechanical testing system (MTS)

the indenter is hung at the center of the cantilever, and just below the indenter is the PDMS sample, which is placed on a motorized translation stage. The stage is controlled by DC servo motors, which can move in three-dimensional space, with a minimum step size of $200nm$; when it moves upwards, the PDMS will punch the indenter which causes the deformations of the cantilever and the PDMS. In the end, we collect the FODS voltage data, along with the stage displacement data. By converting the FODS voltage data into forces and displacements, we can determine the force-deformation relationships.

In the following subsections, we briefly introduce the experimental apparatus and its working principle. Then, we describe the protocols of the three sets of tests and the method of creating the samples. The post-processing follows the similar method in Ferreira's research [**24**]. Cantilever stiffness and voltage-cantilever displacement relationship are obtained from the first two sets of experiments, which are used to calculate the loading forces of deep indentations. In the last set of tests we collect the voltage and stage displacement data. Ultimately, we obtain the force-deformation relationships of the PDMS samples.

1. Experimental apparatus design and setup

Jarod Ferreira clearly introduced the working mechanism of the MTS [**24**]. The main principle is to use the cantilever to measure forces by converting the voltage data of the FODS. Figure 2.2 illustrates how the system operates when a PDMS sample punches the long thin indenter (a pin which is 1.5" in length and 1/16" in diameter). In order to avoid sharpness of the pin tip, we use EPON resin 828 and EPIKURE curing agent 3055 (Figure 2.3) to form a small resin drop on the pin tip as shown in Figure 2.4. First, we mix $1ml$ EPON resin 828 and $1ml$ EPIKURE curing agent 3055. Later, we dip the pin tip into the mixture liquid. In the end, we place the pin in a non-dust chamber at room temperature for 16 hours. After the mixture liquid is fully cured, we use the pin to conduct deep indentation tests.

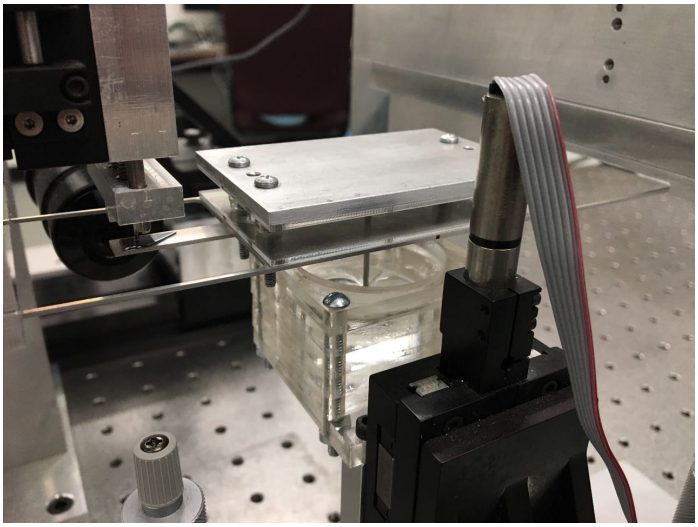

FIGURE 2.2. The deformation of PDMS under deep indentation

FIGURE 2.3. The EPON resin 828 and EPIKURE curing agent 3055

When the indenter punches the PDMS, the cantilever will have a displacement, δ_c. A corresponding voltage change is measured by the FODS. Meanwhile, we collect the displacement of the stage, δ_s. Hence, the deformation of the PDMS sample, δ, is determined. Subtracting the cantilever displacement, or δ_c, from the stage displacement, or δ_s, we thus get:

$$\delta = \delta_s - \delta_c \tag{2.1}$$

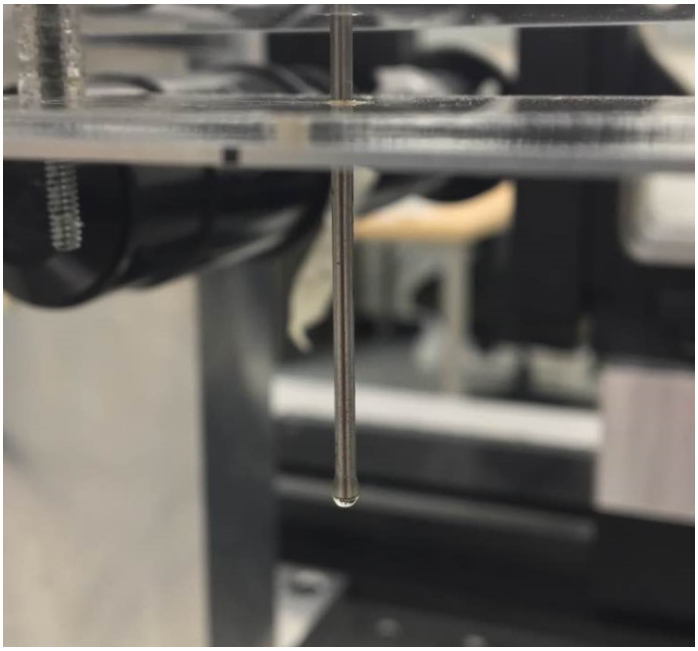

FIGURE 2.4. The tip of long thin indenter

In addition, based on the first two tests, we can determine the cantilever stiffness, K_c (the method to determine K_c is illustrated in section 2.2). Then, multiplying the cantilever displacement and the cantilever stiffness, we obtain the loading force P:

$$P = K_c * \delta_c \tag{2.2}$$

An innovative method is designed to the hold the long thin indenter. Herein, laser cutting technique is utilized to manufacture two identical acrylic plates, whose size are 3"x 2" x 1/16". Next, for each plate, we cut a hole with a diameter the same as that of the indenter. In order to let screws pass through, four holes are created at the corresponding four corners. Between the two plates, standoffs are placed, along with the screws (we present the blueprints of the plate and standoffs in the Appendix A). Furthermore, to vertically place the indenter on the cantilever, we use the following design: the indenter passes through the two center holes of the two plates; next, we use EPON resin 828 and EPIKURE curing agent 3055 to fix the indenter on those two plates.

Before we conduct the experiments, we need to align the indenter with the center of the cantilever. Here, we use a microscope which is fixed on a vertical frame to facilitate the alignment. First, a sign is marked at the central area of the cantilever. Next, we check whether the center of the cantilever is displayed at the visual field center. Later, we place a small rigid sphere indenter on the stage and ensure that the cantilever center is displayed at the visual field center. By doing the alignment process, the indenter and cantilever center are aligned.

Another important prerequisite is that the isolation table surface is required to be horizontal. To achieve this, we adjust the air legs and apply multiple plastic vial bullseyes to check whether its surface is horizontal. After the isolation table is horizontal, all the equipment surfaces are required to be leveled parallel to the isolation table surface. First, the lower surface of the rigid frame is flat and parallel to the isolation table surface when it's mounted on the isolation table. Next, in order to level the stage, we use a flat punch to indent onto a flat PDMS layer attached to the cantilever:

First, we put a flat punch indenter on the stage, whose surface is parallel to the stage surface. Then, we stick a fresh mica layer to the flat punch surface, which makes the punch a very smooth surface that is parallel to the stage surface. In this process, part A and part B of Sylgard 184 are used at a mass ratio of 10:1 and cured at 100°C for 120 minutes to create a PMDS layer. The PDMS layer surface is flat, which is also parallel to the mold bottom surface. Later, the PDMS layer is placed on the lower surface of cantilever central area. We slightly press the flat indenter into the PDMS and adjust the two knobs on the stage to make the PDMS surface flush with the flat punch surface when they come into contact. Finally, the motorized stage is parallel to the isolation table.

2. Cantilever stiffness measurement

We place the weights of known masses on the cantilever center and collect the FODS voltage data. Because the deformations of the cantilever in our experiments

FIGURE 2.5. The Sylgard 527 and 184

are very small, we do a linear fitting to determine the relationship between the force and voltage. Then we obtain the cantilever stiffness which has the unit of N/V. Using the voltage-displacement interpolation (illustrated in section 2.4) we can obtain the cantilever stiffness. Method of choosing a proper cantilever was explained by Ferreira [**24**]. As for our experiments, a cantilever with a stiffness of $2078.8N/m$ is chosen. It is noteworthy that there is a 5% random variation in measurement.

3. Samples preparation

Mechanical properties of samples are crucial for deep indentation tests. The elastic moduli of the samples are required to be around 5-20kPa, and the surfaces should not be easily broken. Sylgard 527 and 184 silicone elastomer bases and elastomer curing agents are chosen to prepare the PDMS samples (Figure 2.5).

To make a pure Sylgard 527 sample, its part A and part B are mixed at a mass ratio of 1:1. However, using a pure Sylgard 527 sample has some drawbacks. First, the pure Sylgard 527 sample is too soft; its elastic modulus is around $1.5kPa$. Also, its surface is very sticky. The indenter will easily pierce into the PDMS. Because of these drawbacks, deep indentation tests can not be conducted on pure Sylgard 527 samples.

To make a pure Sylgard 184 sample, its part A and part B are mixed at a mass ratio of 10:1. One drawback of a pure Sylgard 184 sample is that its elastic modulus of 1.32-2.97MPa [**25**] is extremely large. Although increasing the ratio of Part A can reduce the stiffness, the stiffness is still too great to perform deep indentation tests. Another disadvantage of pure Sylgard 184 is that its surface is vulnerable to damage. Damage is seen after conducting several millimeters' indentation when using a pure Sylgard 184 sample.

To prepare samples with different stiffnesses, we mix the pure Sylgard 527 and 184 at specified ratios. The mixtures of 527 and 184 have great mechanical properties and surface condition. Rachelle N. Palchesko demonstrated that it is feasible to control the elastic modulus without changing surface roughness and material properties [**26**]. Based on his research, we are able to make samples soft enough for our experiments, while their surface properties remain the same. To conduct deep indentations, elastic moduli of soft PDMS samples should be 5-20kPa. So a mass ratio range of pure Sylgard 527 to 184 is chosen as 40:1-60:1. Three different PDMS samples are made by mixing the pure Sylgard 527 and 184 at mass ratios of 40:1, 50:1 and 60:1 (hereon, SYL40, SYL50 and SYL60).

Samples of different stiffnesses are prepared to conduct deep indentation tests. Pure Sylgard 527 and 184 are each prepared as described above. The mixture liquid of pure Sylgard 527 and 184 needs to be stirred for at least 90 seconds to make sure that the two parts are fully mixed. Then we combine these two by the indicated mass ratio followed by an additional mixing. Once completely mixed, the PDMS is poured into the PDMS mold (Figure 2.6). The PDMS bulk is molded in an acrylic cube of 2" in length, 2" in width and 1.1" in height, respectively. There is a cylindrical hollow space in the cube, which is 0.9" in height and 1.8" in diameter, respectively. After a defoaming cycle in the vacuum chamber for at least 30 minutes to make sure there is no air bubbles in the sample, the PDMS sample is cured at 100°C for 45 minutes in an oven placed horizontally on the table. Then we take the PDMS sample out of the oven and place it in a non-dust chamber at room temperature for cooling. After 15

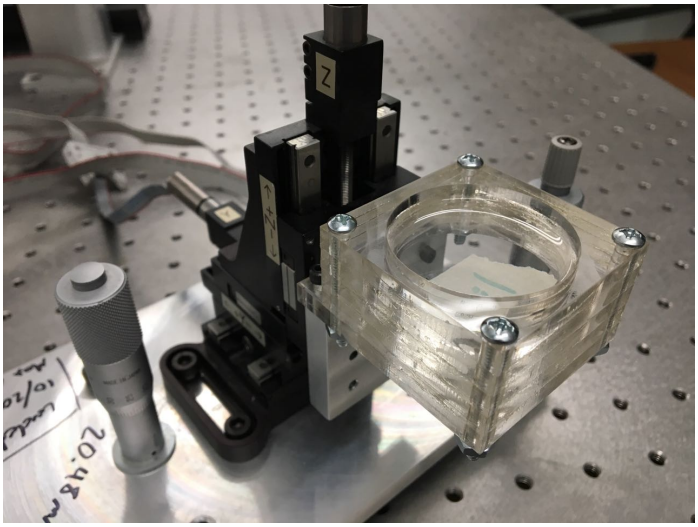

FIGURE 2.6. The PDMS sample mounted on the translation stage

minutes, we visually check the surface condition and inside for bubbles. Flat surface samples without any bubbles inside can then be used to conduct deep indentation experiments.

4. Voltage-displacement interpolation test

A rigid sphere indenter is used to punch the cantilever directly upwards for a sufficient distance, which is from $2.0V$ to $4.75V$ measured by the FODS. Also, we employ a linear fitting to obtain the relationship between voltage and displacement. In result, the FODS voltage data in future tests can be interpolated to the cantilever center displacement.

5. Indentation tests

The PDMS samples with different stiffnesses are tested. For each experiment, one of the PDMS samples is placed on the motorized translation stage, which pushes the PDMS into the pin. Herein, we collect the FODS voltage and stage displacement data.

To control the test processing, a LabVIEW VI program is applied. The stage pushes the PDMS sample in z direction in $50\mu m$ increments. A pause time is introduced between every two loading steps. As a result, the indenter impinges on the

surface of the PDMS and deforms it. The applied force makes the cantilever flex and the cantilever displacement is recorded by the FODS. During the indentation process, at every stage displacement increment we compute the cantilever displacement. Finally, we use the cantilever displacement, cantilever stiffness and stage displacement to compute the displacement of the surface of the PDMS sample beneath the indenter and the force applied by the indenter on the PDMS, and then the force-deformation relationship is obtained.

The indentation test is stopped once any of the following parameters is reached: maximum stage displacement, minimum FODS voltage or maximum FODS voltage. After the loading process, a reverse loading can be conducted continually. In the experiment, voltage and stage displacement data are collected. Next, after the indentation test, we check the surface condition of the PDMS sample to examine whether there is any damage: if no damage exists, we successfully obtain the experimental data that can be applied into the post processing step.

CHAPTER 3

Results and Discussions

Deep indentation tests are conducted on different PDMS samples. The difference between the stage displacement and the cantilever displacement is the deformation of the PDMS sample. By multiplying the cantilever stiffness and the deformation of the cantilever, we know the loading force, and then we can determine the force-deformation relationship of the PDMS.

1. Deep indentation tests on SYL40, SYL50 and SYL60

Three sets of experiments are conducted. SYL40, SYL50 and SYL60 samples are indented deeply by the long thin indenter with a step size at $50\mu m$ and a pause time of $2s$.

Based on these tests, we obtain the mechanical behaviors when PDMS samples are under large deformation. Figures 3.1, 3.2 and 3.3 present the force-displacement relationships corresponding to different PDMS samples.

1.1. Force-displacement curves of SYL40, SYL50 and SYL60.

The black dashed curves in Figures 3.1, 3.2 and 3.3 represent the experimental data of the deep indentation tests on SYL40, SYL50 and SYL60. We use "fitnlm" to do the non-linear fitting based on MATLAB. The fitting function $y = b_1 * x^{b_2}$ is used to reveal the force-deformation relationship. The cyan curves indicate the fitting functions. As shown in the plots, the fitting curves match the experimental curves very well. The coefficients of the fitting functions are shown in the Table 3.1.

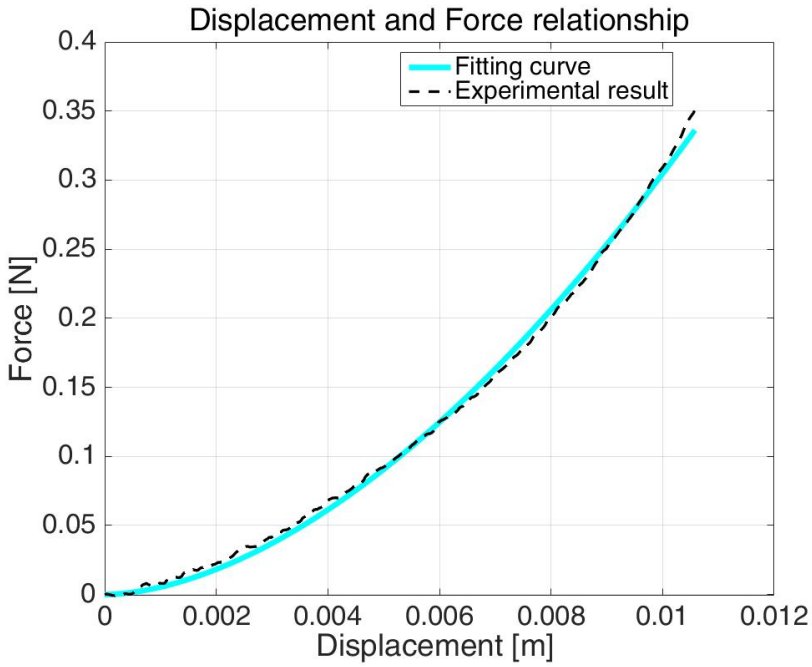

FIGURE 3.1. Force-deformation curve of the SYL40 and fitted by an exponential function

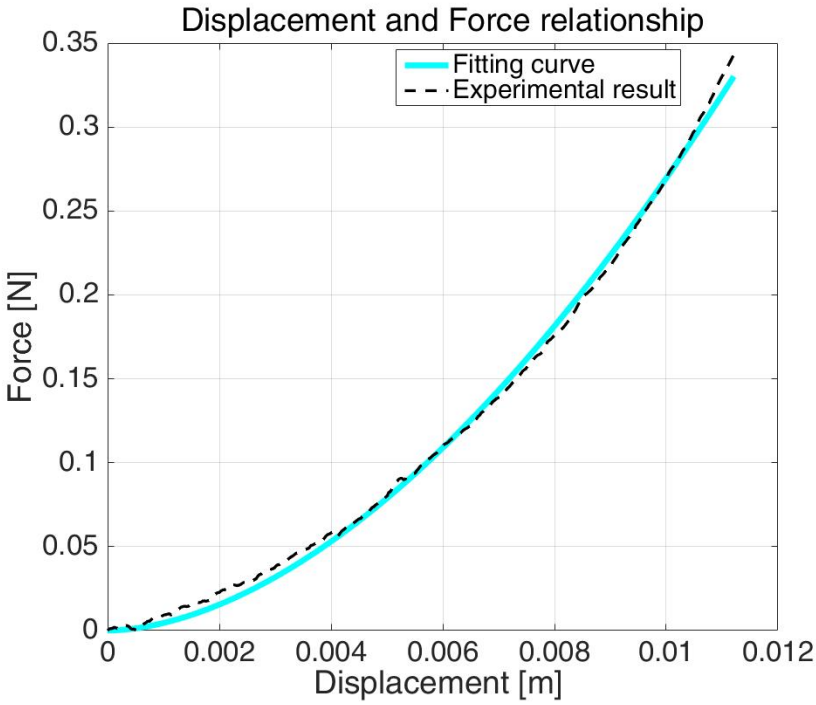

FIGURE 3.2. Force-deformation curve of the SYL50 and fitted by an exponential function

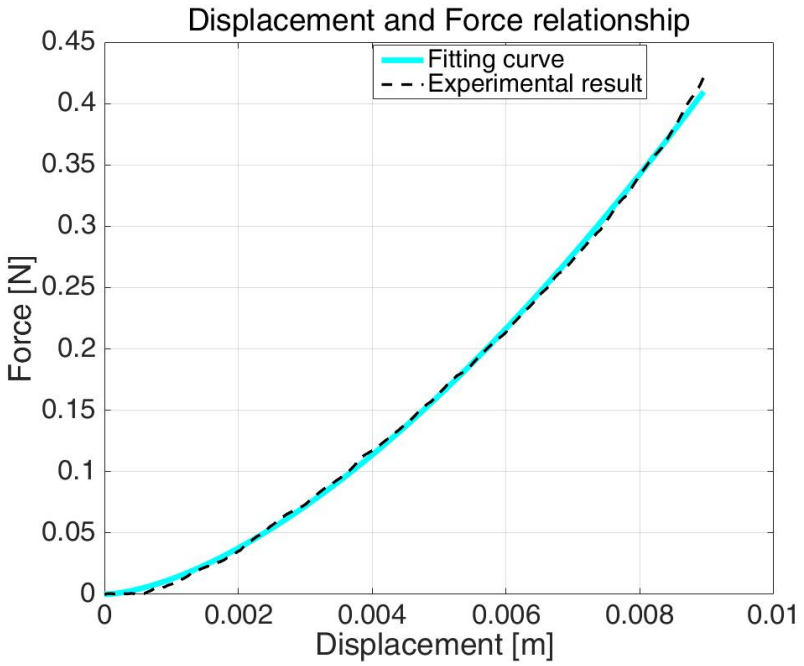

FIGURE 3.3. Force-deformation curve of the SYL60 and fitted by an exponential function

TABLE 3.1. Coefficients of the fitting functions for different PDMS samples (SE: Standard error of the estimate)

Sample	b_1	SE of b_1	b_2	SE of b_2
SYL40	957.35	32.484	1.7486	0.0071079
SYL50	953.89	33.123	1.7744	0.0073671
SYL60	748.86	18.308	1.5927	0.0049325

1.2. Summary.

The experimental data and fitting curves are plotted in Figures 3.1, 3.2 and 3.3. From the experimental curves, we see that at the beginning of the loading process, due to the adhesion effect, there is a small pull-off force. It only happens at the contacting and decontacting moments. After the indenter fully indents into the PDMS sample, the pull-off force disappears. Consequently, the pull-off force has no influence on the

mechanical behavior under deep indentation. It can be seen that the loading force increases smoothly along with the increase of the displacement.

For large indentations on soft PDMS, the force-deformation relations are not linear. An exponential relation is found for PDMS under large deformation. As the coefficients of the fitting functions shown in the Table 3.1, the loading forces increase exponentially as the deformations increase.

The loading force, P, is a function of E^*, R, δ and a:

$$P = P(E^*, R, \delta, a) \tag{3.1}$$

where $E^* = E/(1-\nu^2)$; E, ν, R, a are Young's modulus, Poisson's ratio, the indenter diameter and the contacting area, respectively. For small deformation, Hertz contact is applied and the relationship between the loading force, P, and the deformation, δ, is: $P \propto \delta^{3/2}$ [**27**]. When the deformation is very large, we perform a dimensional analysis to determine the relationship between loading force and the deformation. When $\delta >> R$, the effects of diameter R and the contacting area a decay. Then the loading force, P, is a function of E^*, and δ:

$$P = P(E^*, \delta) \tag{3.2}$$

as the result of the dimensional analysis: $P \propto E^* * \delta^2$. S. Fakhouri demonstrated the force-displacement has a second order under large indentation where the indentation depth is more than 10 times of the indenter diameter [**19**]. This thesis reveals the exponential fitting coefficients locate in the range of 1.5-2 when the indentation depths are 5-7 times of the indenter diameter.

Further experiments of different samples by indenting different depths can be conducted to help deduce the theoretical exponent of the force-deformation formula.

2. Loading and unloading tests on SYL50

2.1. The simple loading and unloading test.

In this experiment, an unloading process is followed after the loading process. The step size and pause time are $50\mu m$ and $2s$, respectively for both the loading

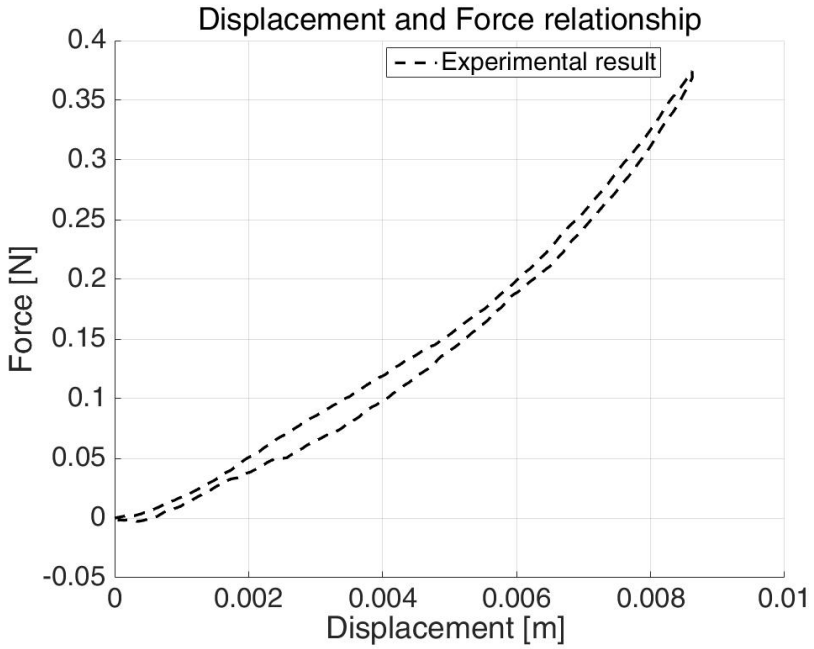

FIGURE 3.4. Force-deformation curves of the SYL50 loading and unloading process

process and the unloading process. The black dashed curves in Figure 3.4 represent the force-displacement relationship during loading process and the unloading process. The ending position of unloading is the same as the starting point of the loading process, which shows that both the loading and unloading are fully elastic. However, there is a hysteresis between loading and unloading.

There are many factors which can cause the hysteresis. In this thesis, we investigate three of the main factors: viscoelasticity, friction and surface roughness. First, as a natural property of hydrogels, viscoelasticity may contribute to the hysteresis. Second, because the compliance of SYL50 is very low, a large deformation will happen even under a small load. When the indenter fully indents into the PDMS sample, as shown in Figure 2.2, the PDMS deforms dramatically. Because the diameter of the indenter is very small and the indentation depth is very large, the PDMS touches the circumferential surface of the indenter. As a result, the surrounding PDMS will compress on the circumferential surface of the indenter and a friction follows. Finally,

the surface roughness of PDMS and the pin tip will cause instability when contact. As a result, an energy loss arises, which may also explain the hysteresis.

In the following subsections, three sets of experiments are conducted to explore the influences of viscoelasticity, friction and surface roughness.

2.2. Viscoelasticity.

2.2.1. *Loading and unloading tests with different pause times on SYL50.*

Three experiments are conducted on SYL50 to explore the influence of viscoelasticity on the mechanical behavior under large deformation. Each experiment has a loading and unloading process. The pause times of the three experiments are $1s$, $2s$ and $5s$, respectively. Except for the pause time, all the other parameters are identical.

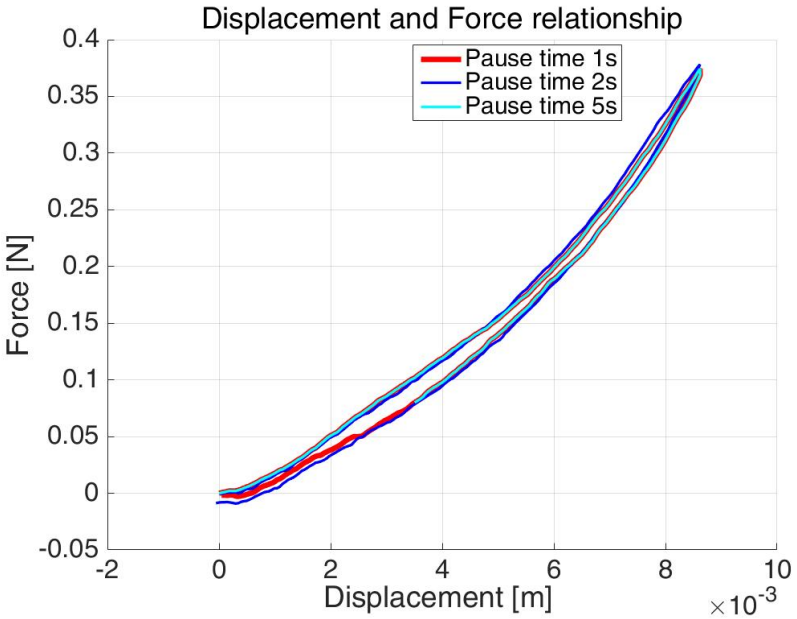

FIGURE 3.5. Force-deformation curves of the SYL50 with different pause times

The hysteresis areas are calculated via the trapezoidal method as shown in Table 3.2, the hystereses are not changed by applying different pause times. We can find that there is no or little contribution from viscoelasticity, or the pause times are not long enough. Then, we conduct another experiment to verify the timescale of viscoelasticity of SYL50.

TABLE 3.2. Hystereses of different pause times

Pause time [s]	1	2	5
Hysteresis [J]	1.1766e-04	1.4623e-04	1.3320e-04

2.2.2. *Relaxing test on SYL50.*

In order to verify the time scale of viscoelasticity, a relaxing test is performed on SYL50. First, the indenter is indented into the SYL50 at $5mm$ in depth. Then, for the next 20 minutes, we record the voltage change. Figure 3.6 shows the force dropping percentage compared with the initial loading force at time 0.

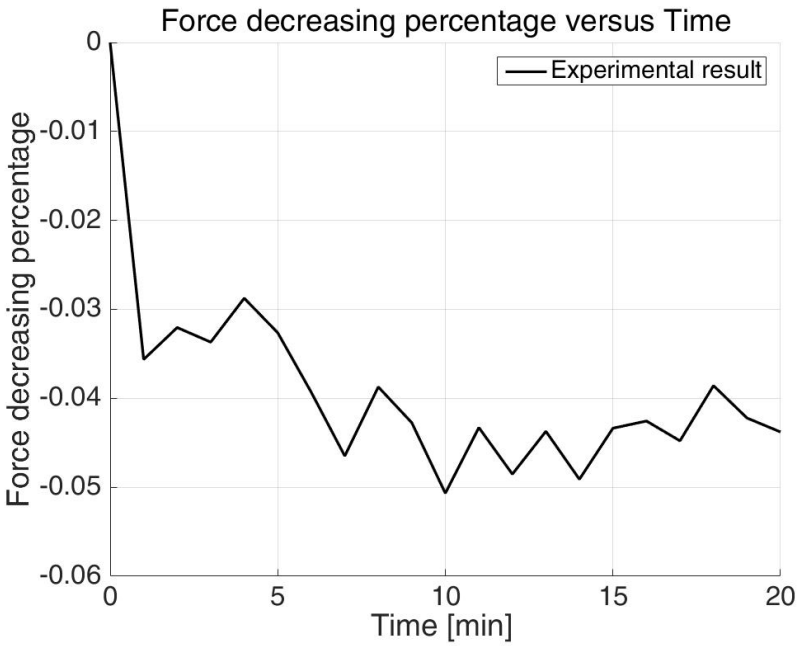

FIGURE 3.6. Relaxing test on SYL50

As shown in the Figure 3.6, the loading force is decreasing as time increases. The curve indicates that the influence of viscoelasticity remains for around 10 minutes. Allowing PDMS more time to get to static state dramatically reduces the effect of viscoelasticity. The result of the relaxing test shows that the timescale of viscoelasticity of SYL50 is around 10 minutes.

Consequently, a quantitative pause time is determined from the test. For example, a quantitative pause time larger than 10 minutes can reduce the effect of viscoelasticity

for a SYL50 sample. In the future, this method can be applied to other soft materials when performing deep indentation tests.

2.3. Surface conditions.

The hysteresis may also result from the side friction and energy loss. Under large indentation when the indenter indents deeper than its diameter, the soft PDMS contacts the circumferential surface of the indenter. Then a side friction is generated which may contribute to the hysteresis. Also, the instability caused by surface roughness during contact can result in the hysteresis.

Two experiments are run on SYL50 to explore the influences of surface roughness and friction on its mechanical behavior under large deformation. We use the same SYL50 for both experiments. The first experiment is conducted directly without changing any PDMS surface conditions. While the second is conducted by spraying the dish washing liquid on its surface evenly. 10% dish washing soap is dissolved in the isopropanol liquid which is made by mixing 75% isopropanol and 25% distilled water. The soap liquid can reduce the surface roughness, which will reduce the friction and the energy loss. To maximize the smoothing effect, we spray the soap liquid twice. 15 minutes after the first spraying, we spray again and immediately use the PDMS sample to do the deep indentation. In this test, the pause time is set as $2s$ in order to compare with the result from the previous test, which only differs in the surface roughness of the PDMS while other parameters are identical. All the other parameters are the same. The force-displacement curves are shown in Figure 3.7.

TABLE 3.3. Hystereses of different surface conditions

Surface treatment	No	Yes
Hysteresis area $[J]$	1.4623e-04	1.0800e-04

As shown in Table 3.3, comparing the two curves, there is a small decrease of hysteresis after spraying the soap liquid on the PDMS surface. There are two interpretations which can explain the small decrease. First, the friction and the surface

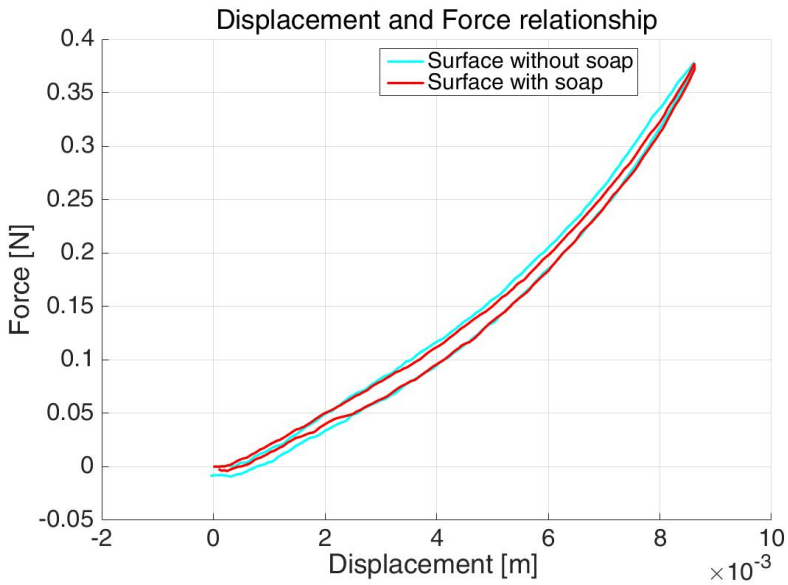

FIGURE 3.7. Force-deformation curves of the SYL50 with different surface conditions

roughness contribute to the hysteresis, however, their effects are very small. Second, because the initial roughnesses of both the PDMS and the pin surfaces are very small, the soap liquid only makes their surface a little smoother. Consequently, the small difference between the initial roughness and the reduced roughness can only reduce the hysteresis by a very small amount.

Furthermore, the soap liquid generates capillary forces on the PDMS surface. The capillary forces also contribute to the hysteresis. Further research can be done to investigate the influence of capillary forces on hysteresis.

CHAPTER 4

Conclusions

We use a long thin indenter to conduct deep indentation tests on three different PDMS samples: SYL40, SYL50 and SYL60 in order to find the force-deformation relationship of PDMS under large deformation. The force-deformation relation is not linear under deep indentation. An exponential relation and the fitting coefficients are discovered.

We also conduct an unloading test which follows the loading process. There is a hysteresis between the loading and unloading curves. Three potential factors of viscoelasticity, friction and surface roughness are discussed. We employ three sets of experiments to investigate the three factors. From the results, we demonstrate that the timescale of viscoelasticity of SYL50 is around 10 minutes. The surface roughness and friction also have a small contribution to the hysteresis.

APPENDIX A

Blue prints

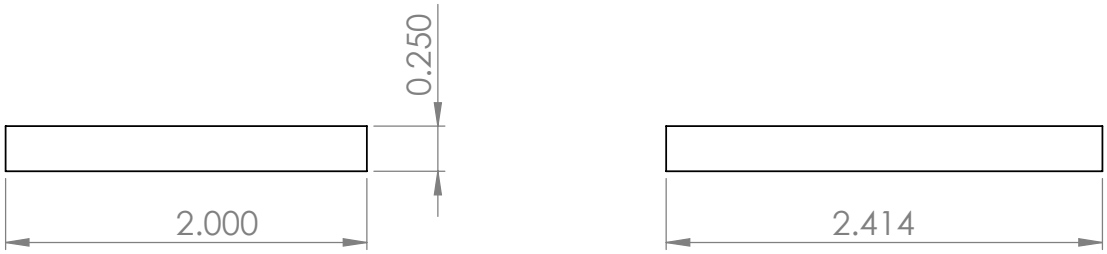

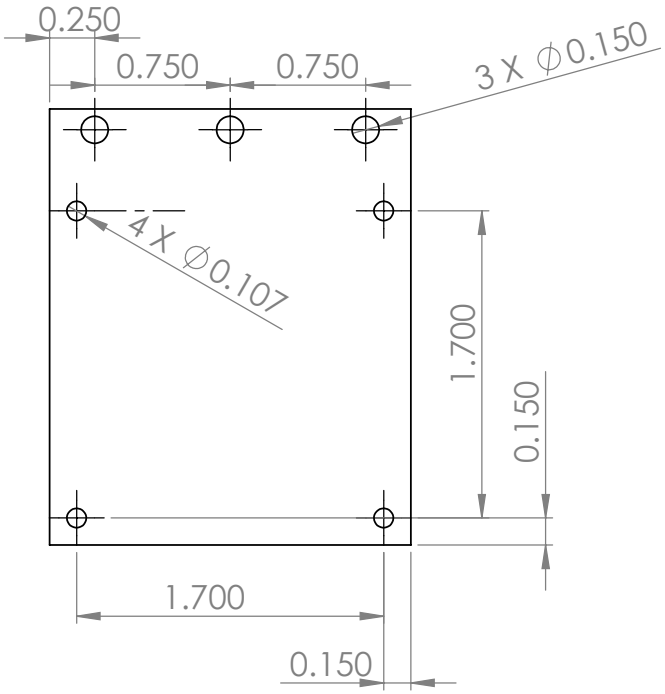

UNLESS OTHERWISE SPECIFIED: DIMENSIONS ARE IN MILLIMETERS SURFACE FINISH: TOLERANCES: LINEAR: ANGULAR:		FINISH:			DEBUR AND BREAK SHARP EDGES	DO NOT SCALE DRAWING	REVISION
	NAME	SIGNATURE	DATE			TITLE:	
DRAWN							
CHK'D							
APPV'D							
MFG							
Q.A				MATERIAL:		DWG NO. Base_First_cut	A4
				WEIGHT:		SCALE:1:1	SHEET 1 OF 1

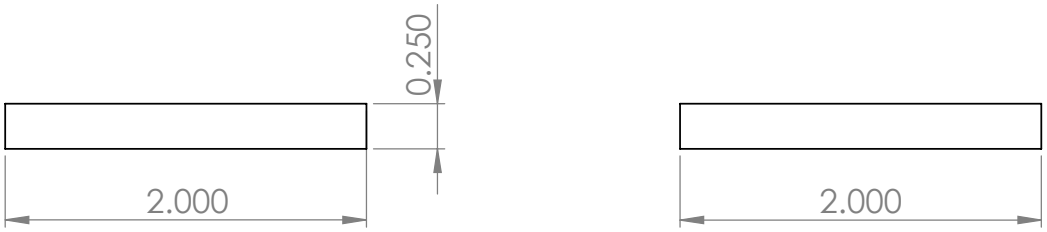

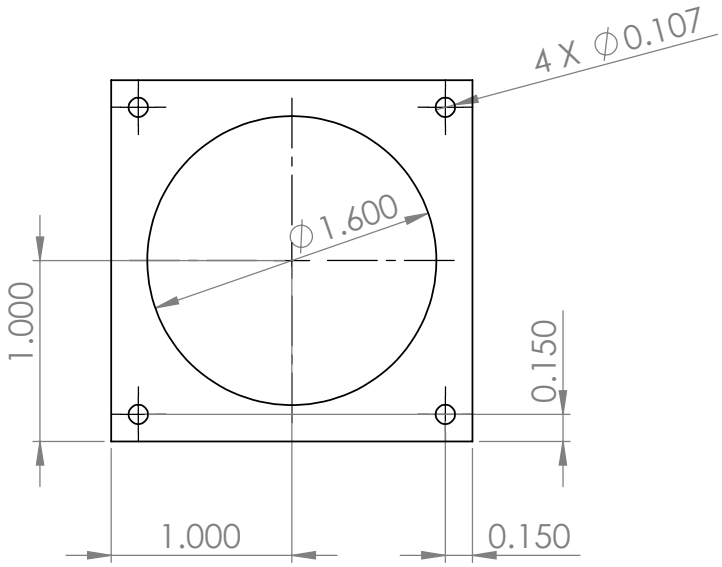

UNLESS OTHERWISE SPECIFIED: DIMENSIONS ARE IN MILLIMETERS SURFACE FINISH: TOLERANCES: LINEAR: ANGULAR:	FINISH:		DEBUR AND BREAK SHARP EDGES			DO NOT SCALE DRAWING	REVISION
	NAME	SIGNATURE	DATE			TITLE:	
DRAWN							
CHK'D							
APPV'D							
MFG							
Q.A				MATERIAL:		DWG NO. PDMS-layer	A4
				WEIGHT:		SCALE:1:1	SHEET 1 OF 1

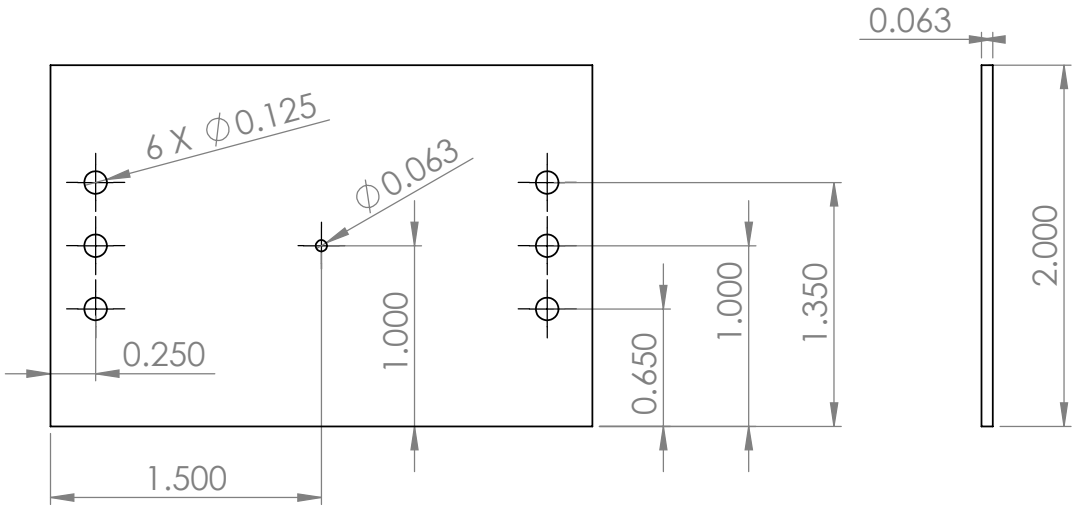

UNLESS OTHERWISE SPECIFIED: DIMENSIONS ARE IN MILLIMETERS SURFACE FINISH: TOLERANCES: LINEAR: ANGULAR:		FINISH:			DEBUR AND BREAK SHARP EDGES	DO NOT SCALE DRAWING	REVISION
	NAME	SIGNATURE	DATE			TITLE:	
DRAWN							
CHK'D							
APPV'D							
MFG							
Q.A				MATERIAL:		DWG NO. Plate	A4
				WEIGHT:		SCALE:1:1	SHEET 1 OF 1

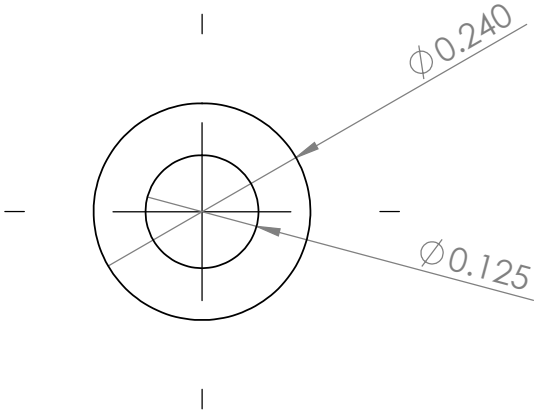

UNLESS OTHERWISE SPECIFIED: DIMENSIONS ARE IN MILLIMETERS SURFACE FINISH: TOLERANCES: LINEAR: ANGULAR:		FINISH:			DEBUR AND BREAK SHARP EDGES	DO NOT SCALE DRAWING	REVISION
	NAME	SIGNATURE	DATE			TITLE:	
DRAWN							
CHK'D							
APPV'D							
MFG							
Q.A				MATERIAL:		DWG NO. Standoff	A4
				WEIGHT:		SCALE:5:1	SHEET 1 OF 1

Bibliography

[1] G. Rubio, N. Agrait, and S. Vieira, "Atomic-sized metallic contacts: mechanical properties and electronic transport," *Physical review letters*, vol. 76, no. 13, p. 2302, 1996.

[2] B. Ji and H. Gao, "Mechanical properties of nanostructure of biological materials," *Journal of the Mechanics and Physics of Solids*, vol. 52, no. 9, pp. 1963–1990, 2004.

[3] P.-Y. Chen, A. Lin, Y.-S. Lin, Y. Seki, A. Stokes, J. Peyras, E. Olevsky, M. Meyers, and J. McKittrick, "Structure and mechanical properties of selected biological materials," *Journal of the Mechanical Behavior of Biomedical Materials*, vol. 1, no. 3, pp. 208–226, 2008.

[4] S. Bechtle, S. F. Ang, and G. A. Schneider, "On the mechanical properties of hierarchically structured biological materials," *Biomaterials*, vol. 31, no. 25, pp. 6378–6385, 2010.

[5] Y.-c. Fung, *Biomechanics: mechanical properties of living tissues*. Springer Science & Business Media, 2013.

[6] H. Saraf, K. Ramesh, A. Lennon, A. Merkle, and J. Roberts, "Mechanical properties of soft human tissues under dynamic loading," *Journal of biomechanics*, vol. 40, no. 9, pp. 1960–1967, 2007.

[7] T. Kokubo, H.-M. Kim, and M. Kawashita, "Novel bioactive materials with different mechanical properties," *Biomaterials*, vol. 24, no. 13, pp. 2161–2175, 2003.

[8] C. M. Buffinton, K. J. Tong, R. A. Blaho, E. M. Buffinton, and D. M. Ebenstein, "Comparison of mechanical testing methods for biomaterials: Pipette aspiration, nanoindentation, and macroscale testing," *journal of the mechanical behavior of biomedical materials*, vol. 51, pp. 367–379, 2015.

[9] I. Engelberg and J. Kohn, "Physico-mechanical properties of degradable polymers used in medical applications: a comparative study," *Biomaterials*, vol. 12, no. 3, pp. 292–304, 1991.

[10] C.-Y. Huang, A. Stankiewicz, G. A. Ateshian, and V. C. Mow, "Anisotropy, inhomogeneity, and tension–compression nonlinearity of human glenohumeral cartilage in finite deformation," *Journal of biomechanics*, vol. 38, no. 4, pp. 799–809, 2005.

[11] W. C. Oliver and G. M. Pharr, "An improved technique for determining hardness and elastic modulus using load and displacement sensing indentation experiments," *Journal of materials research*, vol. 7, no. 06, pp. 1564–1583, 1992.

[12] J.-Y. Rho, T. Y. Tsui, and G. M. Pharr, "Elastic properties of human cortical and trabecular lamellar bone measured by nanoindentation," *Biomaterials*, vol. 18, no. 20, pp. 1325–1330, 1997.

[13] J. Kinney, S. Marshall, and G. Marshall, "The mechanical properties of human dentin: a critical review and re-evaluation of the dental literature," *Critical Reviews in Oral Biology & Medicine*, vol. 14, no. 1, pp. 13–29, 2003.

[14] D. Ebenstein and L. Pruitt, "Nanoindentation of soft hydrated materials for application to vascular tissues," *Journal of Biomedical Materials Research Part A*, vol. 69, no. 2, pp. 222–232, 2004.

[15] K. R. Shull, "Contact mechanics and the adhesion of soft solids," *Materials Science and Engineering: R: Reports*, vol. 36, no. 1, pp. 1–45, 2002.

[16] P. Warren, "Determining the fracture toughness of brittle materials by hertzian indentation," *Journal of the European Ceramic Society*, vol. 15, no. 3, pp. 201–207, 1995.

[17] K.-C. Wu and H.-I. You, "Determination of solid material elastic modulus and surface energy based on jkr contact model," *Applied surface science*, vol. 253, no. 20, pp. 8530–8537, 2007.

[18] Y. Cao, D. Yang, and W. Soboyejoy, "Nanoindentation method for determining the initial contact and adhesion characteristics of soft polydimethylsiloxane," *Journal of Materials Research*, vol. 20, no. 08, pp. 2004–2011, 2005.

[19] S. Fakhouri, S. B. Hutchens, and A. J. Crosby, "Puncture mechanics of soft solids," *Soft matter*, vol. 11, no. 23, pp. 4723–4730, 2015.

[20] P. Du, I.-K. Lin, H. Lu, X. Zhang, *et al.*, "Characterization on the viscoelastic property of pdms in the frequency domain," in *MRS Proceedings*, vol. 1301, pp. mrsf10–1301, Cambridge Univ Press, 2011.

[21] W. Deng and H. Kesari, "Molecular statics study of depth-dependent hysteresis in nano-scale adhesive elastic contacts," *Modelling and Simulation in Materials Science and Engineering*, vol. 25, no. 5, p. 055002, 2017.

[22] H. Kesari, J. C. Doll, B. L. Pruitt, W. Cai, and A. J. Lew, "Role of surface roughness in hysteresis during adhesive elastic contact," *Philosophical Magazine & Philosophical Magazine Letters*, vol. 90, no. 12, pp. 891–902, 2010.

[23] H. Kesari and A. J. Lew, "Effective macroscopic adhesive contact behavior induced by small surface roughness," *Journal of the Mechanics and Physics of Solids*, vol. 59, no. 12, pp. 2488–2510, 2011.

[24] J. N. Ferreira, "Adhesive contact experiments with non-linear model fitting," May 2016.

[25] I. Johnston, D. McCluskey, C. Tan, and M. Tracey, "Mechanical characterization of bulk sylgard 184 for microfluidics and microengineering," *Journal of Micromechanics and Microengineering*, vol. 24, no. 3, p. 035017, 2014.

[26] R. N. Palchesko, L. Zhang, Y. Sun, and A. W. Feinberg, "Development of polydimethylsiloxane substrates with tunable elastic modulus to study cell mechanobiology in muscle and nerve," *PloS one*, vol. 7, no. 12, p. e51499, 2012.

[27] S. Muthukumar and R. DesRoches, "A hertz contact model with non-linear damping for pounding simulation," *Earthquake engineering & structural dynamics*, vol. 35, no. 7, pp. 811–828, 2006.